Transitions to Synchrony in Coupled Bursting Neurons

Mukeshwar Dhamala,[1] Viktor K. Jirsa,[1,2] and Mingzhou Ding[1,3]

[1]*Center for Complex Systems and Brain Sciences, Florida Atlantic University, Boca Raton, Florida 33431, USA*
[2]*Department of Physics, Florida Atlantic University, Boca Raton, Florida 33431, USA*
[3]*Department of Mathematical Sciences, Florida Atlantic University, Boca Raton, Florida 33431, USA*

(Received 8 September 2003; revised manuscript received 14 November 2003; published 15 January 2004)

Certain cells in the brain, for example, thalamic neurons during sleep, show spike-burst activity. We study such spike-burst neural activity and the transitions to a synchronized state using a model of coupled bursting neurons. In an electrically coupled network, we show that the increase of coupling strength increases incoherence first and then induces two different transitions to synchronized states, one associated with bursts and the other with spikes. These sequential transitions to synchronized states are determined by the zero crossings of the maximum transverse Lyapunov exponents. These results suggest that synchronization of spike-burst activity is a multi-time-scale phenomenon and burst synchrony is a precursor to spike synchrony.

DOI: 10.1103/PhysRevLett.92.028101 PACS numbers: 87.19.La, 05.45.Xt, 84.35.+i

The phenomenon of neuronal spike-burst activity is characterized by a recurrent transition between rest state and firing state with a burst of multiple spikes. This activity is a multi-time-scale phenomenon and is caused by a slow process (burst) modulating the fast action-potential firing (spike). Certain cells in the mammal brain, for example, neurons in the thalamus during periods of drowsiness, inattentiveness, and sleep, are known to exhibit spike-burst activity [1–4]. The slow (<1 Hz) oscillations, observed in the electroencephalographic recordings of naturally sleeping humans and other mammals, are considered to be the result of a synchronized spike-burst activity of billions of neurons in the brain [4,5]. Midbrain dopaminergic neurons, which have great importance in different aspects of brain function such as reward-mediated learning, movement control, cognition, and motivation [6], also exhibit two modes of action-potential firing: spike firing and burst firing [7,8]. Some clinical disorders, such as Parkinson's disease, schizophrenia, and drug addiction, are found to be originated from some imbalance in these neurons [9–11]. Interestingly, some types of epileptic seizures are also believed to depend on rhythmic burst firing in the thalamic and thalamocortical circuits [12–14]. Thus, the study of synchronization and desynchronization of neuronal spike-burst behaviors from biophysical models may help us understand further the information processing in the brain and even the origins of certain mental disorders.

Synchronization of neurons with spike-burst activity may involve synchrony of individual spikes and/or synchrony of bursts, or both. There have been some theoretical studies on the classification of bursting behaviors from neuron models [15,16]. The bursting activity, which is typically viewed as being the result of interaction between the multi-time-scale (fast and slow) subsystems and the slow subsystem, is considered responsible for switching the dynamics of the fast subsystem between rest and bursting states. In a coupled system, burst synchronization is often found easier to achieve than individual spike synchronization. However, the question of systematic transitions to synchrony and the order of synchronization in multi-time-scale systems of coupled oscillators remains unexplored.

In a coupled system of certain chaotic oscillators, as the coupling strength is increased from zero, the oscillations become less and less incoherent and finally completely coherent —first, synchronization in phase and then synchronization in amplitude emerge [17,18]. A recent work [19] involving coupled Lorenz attractors revealed that the oscillations can be more incoherent as a result of coupling as measured by Lyapunov exponents. The authors suggest that this phenomenon is causally related to the existence of double scrolls in the Lorenz attractor. One can view multiple scrolls as a geometric analog of multiple inherent time scales in the system. The question of general interest is then about the effect of different time scales (as in neurons) and coupling strength on coherence of oscillations in a coupled system.

The purpose of this Letter is to investigate this question in the context of neuronal spike-burst behaviors. Using a coupled system of Hindmarsh-Rose (HR) [20,21] neurons, we present evidence that the coupling strength can increase incoherence first and then induce two different transitions to synchronized states, one associated with burst (slow time-scale dynamics) and the other with spikes (fast time-scale dynamics).

A multi-time-scale dynamical system (for example, a neuron with spike-burst behaviors) can be written in a singularly perturbed form: $\dot{\mathbf{x}} = f(\mathbf{x}, \mathbf{y})$, $\dot{\mathbf{y}} = \mu g(\mathbf{x}, \mathbf{y})$, where $\mathbf{x}$ is a vector of fast variables, $\mathbf{y}$ is a vector of slow variables that modulates the fast activity, and $\mu \ll 1$ is a ratio of fast/slow time scales. In such a system, one usually observes an almost instant jump in $\mathbf{x}$ components followed by a finite speed motion in the $\mathbf{y}$ components. Setting $\mu = 0$ yields the equation $\dot{\mathbf{x}} = f(\mathbf{x}, \mathbf{y})$ for the fast subsystem with a constraint, $\dot{\mathbf{y}} = \mathbf{0}$. Equivalently,

rescaling time with $\tau = \mu t$ and setting $\mu = 0$, one obtains the equation for the slow subsystem as $f(\mathbf{x}, \mathbf{y}) = \mathbf{0}$, $\mathbf{y}' = g(\mathbf{x}, \mathbf{y})$, where $' = d/d\tau$. Here $f(\mathbf{x}, \mathbf{y}) = \mathbf{0}$ represents the slow manifold. One can look at the slow and fast subsystems separately and find their common asymptotic state to estimate the state of the full system.

As an example of a singularly perturbed system, we consider the Hindmarsh-Rose neuron described by the following equations of motion [21]: $\dot{x} = y - ax^3 + bx^2 - z + I_{\text{ext}}$, $\dot{y} = c - dx^2 - y$, $\dot{z} = r[s(x - x_0) - z]$, where x is the membrane potential, y is associated with the fast current, Na^+ or K^+, and z with the slow current, for example, Ca^{2+}. Here $a = 1.0$, $b = 3.0$, $c = 1.0$, $d = 5.0$, $s = 4.0$, $r = 0.006$, $x_0 = -1.60$, and I_{ext} is the external current input. x, y are fast variables and z is a slow variable. r is the ratio of fast/slow time scales. This system exhibits a multi-time-scale spike-burst chaotic behavior for $2.92 < I_{\text{ext}} < 3.40$, as shown in the bifurcation diagram (Fig. 1), where the time interval (Δt) between successive spikes is plotted against I_{ext}. The inset is a time series of membrane potential (x) showing spike-burst activity at $I_{\text{ext}} = 3.2$. Now we consider two HR neurons coupled linearly via x component as follows: $\dot{x}_i = y_i - ax_i^3 + bx_i^2 - z_i + I_{\text{ext}} + \epsilon(x_j - x_i)$, $\dot{y}_i = c - dx_i^2 - y_i$, and $\dot{z}_i = r[s(x_i - x_0) - z_i]$, where $\epsilon \geq 0$ is the coupling strength, and $i = 1, 2$, $j = 2, 1$ are the indices. The synchronized state will then be represented by:

$$\dot{x} = y - ax^3 + bx^2 - z + I_{\text{ext}}, \tag{1}$$

$$\dot{y} = c - dx^2 - y, \tag{2}$$

$$\dot{z} = r[s(x - x_0) - z], \tag{3}$$

as the differences $|x_1 - x_2|$, $|y_1 - y_2|$, $|z_1 - z_2|$ vanish in the limit of $t \to \infty$. This occurs when the synchronization manifold becomes completely stable. If we now transform to $x_\perp = x_1 - x_2$, $y_\perp = y_1 - y_2$, and $z_\perp = z_1 - z_2$, in the limit when these variables are very small ($x_1^2 - x_2^2 \approx 2xx_\perp$ and $x_1^3 - x_2^3 \approx 3x^2x_\perp$), the motion transverse to the synchronization manifold can be described by the following equations:

$$\dot{x}_\perp = y_\perp - 3ax^2x_\perp + 2bxx_\perp - z_\perp - 2\epsilon x_\perp, \tag{4}$$

$$\dot{y}_\perp = -2dxx_\perp - y_\perp, \tag{5}$$

$$\dot{z}_\perp = r(sx_\perp - z_\perp). \tag{6}$$

The solution of Eqs. (4)–(6) determines the stability of the synchronized states. The minimal condition for stability of the synchronized state represented by Eqs. (1)–(3) is that the Lyapunov exponents associated with Eqs. (4)–(6) be negative for the transverse subsystem. By solving Eqs. (4)–(6) in combination with Eqs. (1)–(3), we determine the transverse Lyapunov exponents, two of those shown in Fig. 2. As the coupling strength is increased from zero, the initially zero exponent starts to increase, reaches a peak, and then starts to decrease along with the other positive exponent. These exponents cross zeros at two different coupling strengths and both become negative. It implies that coupling may not always increase coherence. Instead, in a multi-time-scale system of coupled oscillators, a low coupling strength makes the system more incoherent and higher coupling strengths can synchronize the slow subsystem or both the slow and fast subsystems. Figure 3 underscores this point. The first transition occurs at $\epsilon = 0.45$ and the second transition at $\epsilon = 0.50$ corresponding, respectively,

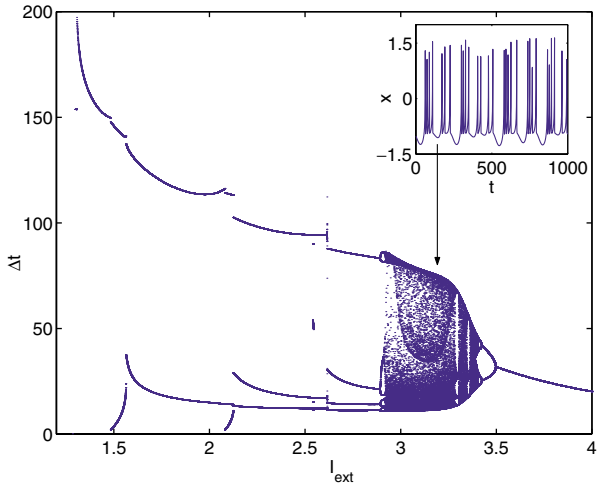

FIG. 1 (color online). The bifurcation diagram for a Hindmarsh-Rose neuron: interspike interval (Δt) versus external current (I_{ext}). The inset shows the time series of a spike-burst activity of membrane potential (x) at $I_{\text{ext}} = 3.2$.

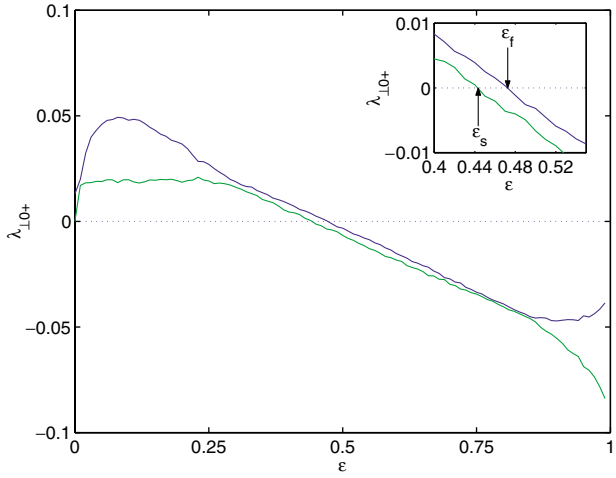

FIG. 2 (color online). Initially zero and positive transverse Lyapunov exponents ($\lambda_{\perp 0+}$) versus coupling strength (ϵ). The initial increase of the zero Lyapunov exponent with the coupling strength is evidence that coupling may not always increase the degree of coherence of oscillations in a coupled system, especially in multi-time-scale dynamical systems. The inset is the blowup of the portion of the plot near the transitions at $\epsilon_s \approx 0.45$ and $\epsilon_f \approx 0.50$, where ϵ_s and ϵ_f correspond to the onsets of burst synchrony and spike synchrony, respectively.

to the synchronization of the slow and fast oscillations of the coupled system. All the transverse variables $(x_\perp, y_\perp, z_\perp)$ diverge from zero with time at $\epsilon = 0.40$ [shown in Figs. 3(a) and 3(b)]. Only $x_\perp$ and $y_\perp$, which are associated with the fast dynamics, diverge at $\epsilon = 0.40$, and the variable associated with the slow dynamics, $z_\perp$, remains close to zero [shown in Figs. 3(c) and 3(d)]. Figures 3(e) and 3(f) show that $x_\perp$, $y_\perp$, and $z_\perp$ all converge to zero at $\epsilon = 0.52$.

We now consider the slow subsystem and estimate the coupling strength for its transition to the synchronized state with an analytical approach. The equations obtained by rescaling time with $\tau = rt$ and setting $r \to 0$ in Eqs. (1)–(6) represent the slow subsystem and are as follows: $z' = s(x - x_0) - z$ and $z'_\perp = sx_\perp - z_\perp$, with the constraints $0 = c - (d - b)x^2 - ax^3 - z + I_{\text{ext}}$ and $0 = -[2(d - b)x + 3ax^2 + 2\epsilon]x_\perp - z_\perp$. Eliminating $x_\perp$ from these equations, we obtain

$$z'_\perp = \left[\frac{1}{\gamma(x, \epsilon)} - 1\right] z_\perp, \tag{7}$$

where $\gamma(x, \epsilon) = -[2(d - b)x + 3ax^2 + 2\epsilon]/s$. The synchronized state on the slow time scale will be stable if $\{[1/\gamma(x, \epsilon)] - 1\} \leq 0$. On the other hand, we do not pose a stability constraint on $x_\perp$ and $y_\perp$, and thus we investigate only the onset of burst synchrony. Using the asymptotic state of the full system and the first equation of the constraints, we first parametrize x on the slow manifold by a numerical fit. Then, for the entire range $0 \leq \epsilon \leq 1$, we calculate $\gamma(x, \epsilon)$. The result shows that $\{[1/\gamma(x, \epsilon)] - 1\}$ changes sign from positive to negative at $\epsilon = 0.45$, which is in excellent agreement with $\epsilon_s = 0.45$, the first transition in Fig. 2. This alternative analytical approach also confirms that the first transition in Fig. 2 is associated with the slow subsystem.

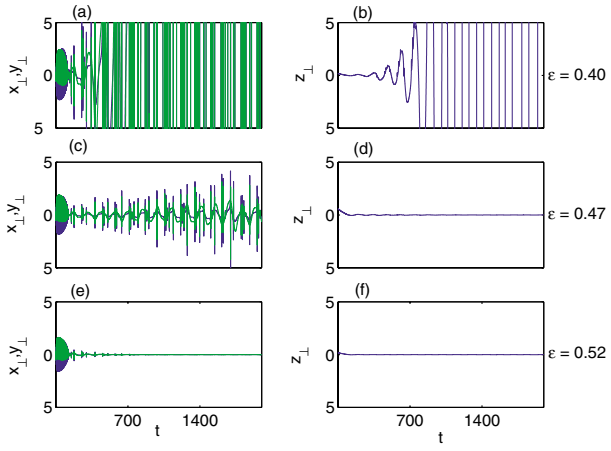

FIG. 3 (color online). Variations $(x_\perp, y_\perp, z_\perp)$ transverse to t he synchronization manifold. (a),(b) $x_\perp, y_\perp, z_\perp$ all diverge from zero at $\epsilon = 0.40 < \epsilon_s$. (c),(d) At $\epsilon = 0.47 < \epsilon_f$, only $z_\perp$ stays bounded around zero, indicating synchrony only on the slow time scale. (e),(f) All the variations $(x_\perp, y_\perp, z_\perp)$ damp out to zero at $\epsilon = 0.52 > \epsilon_f$, resulting in the system in full synchrony.

As the ratio $(r \ll 1)$ of fast/slow time scales in Eqs. (1)–(3) is increased, the time interval between bursts start to change. At higher values of r, the average interburst interval is of the same order as the average interspike interval. Figure 4 shows how r changes the onsets of burst and spike synchrony. As $r \to 1$, these two transitions merge into one. These results consistently imply that multi-time-scale dynamical systems have different regimes of synchronization for different time scales.

The calculation of Lyapunov exponents can be done for a network of N neurons in a similar way. Figure 5 shows two of the maximum transverse Lyapunov exponents in an electrically coupled network of eight neurons. The numerical simulation was carried out by taking the Jacobian matrix for the full coupled system. The feature of two transition points as in a two-neuron system can also be seen here. In general, for an N-neuron network, one can follow a similar scheme used by Pecora and Carrol in Ref. [22] to look at the variations transverse to the synchronization manifold. For example, let us consider an N-neuron network described by the following equation:

$$\dot{\mathbf{x}}_i = \mathbf{F}(\mathbf{x}_i) + \epsilon \sum_j G_{ij} \mathbf{H}(\mathbf{x}_j), \tag{8}$$

where $\mathbf{x}_i$ is the dynamical variable vector (x_i, y_i, z_i) for site i in an N-oscillator array. The isolated dynamics for each neuron is $\dot{\mathbf{x}}_i = \mathbf{F}(\mathbf{x}_i)$. Here ϵ is the coupling strength, $\mathbf{H}: R^3 \to R^3$ is the coupling function, and $\mathbf{G}$ is an $N \times N$ matrix which determines neuron-to-neuron coupling. The $N - 1$ constraints $\mathbf{x}_1 = \mathbf{x}_2 = \ldots = \mathbf{x}_N$ define the synchronization manifold. For the invariance of the synchronization manifold, the rows of G_{ij} are chosen

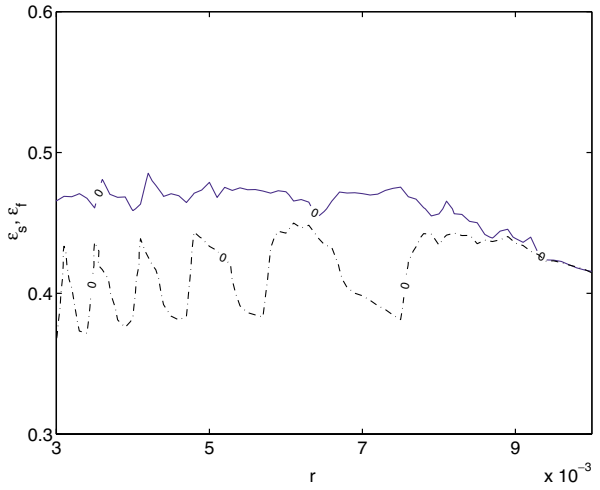

FIG. 4 (color online). (ϵ_s, ϵ_f) at $\lambda_{\perp 0+} = 0$ versus r (dashed line for ϵ_s and solid line for ϵ_f). As the ratio (r) of fast/slow time scales is increased, the two transitions for synchronization merge into one.

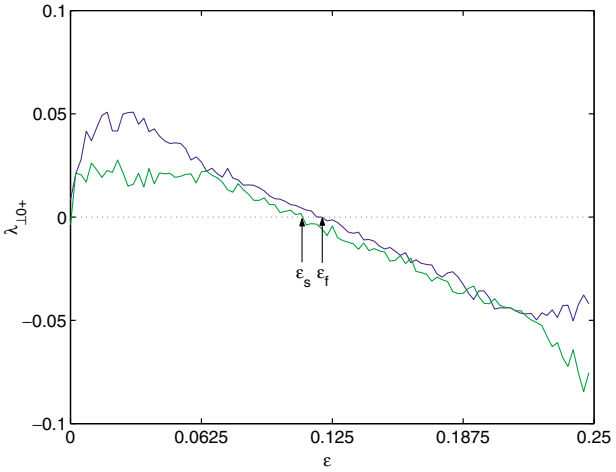

FIG. 5 (color online). $\lambda_{\perp 0+}$ versus ϵ in a network of eight neurons. Here also, the first two maximum transverse Lyapunov exponents cross zero on the ϵ axis at different points: $\epsilon_s \approx 0.11$ and $\epsilon_f \approx 0.12$.

such that $\sum_{j=1}^{N} G_{ij} = 0$. Considering perturbations to the synchronized state $\mathbf{x}$ and diagonalizing $\mathbf{G}$, one obtains the generic block-diagonalized variational equation for the transverse directions as follows:

$$\dot{\boldsymbol{\xi}} = D\mathbf{F}(\mathbf{x})\boldsymbol{\xi} + (\alpha + \sqrt{-1}\beta)D\mathrm{H}(\mathbf{x})\boldsymbol{\xi},$$

where $(\alpha + \sqrt{-1}\beta)$ is an eigenvalue of $\epsilon\mathbf{G}$. $D\mathbf{F}(\mathbf{x})$ is the Jacobian matrix evaluated on the synchronization manifold and $D\mathbf{H}(\mathbf{x})$ is a 3×3 matrix that determines which of the oscillator components are coupled. For example, for x component coupling in a network of Hindmarsh-Rose neurons, only the first element of the 3×3 matrix is 1 and all the others are 0. Separating $\boldsymbol{\xi}$ into real part $\boldsymbol{\xi}_r$ and imaginary part $\boldsymbol{\xi}_i$, we get

$$\dot{\boldsymbol{\xi}}_r = [D\mathbf{F}(\mathbf{x}) + \alpha D\mathbf{H}(\mathbf{x})]\boldsymbol{\xi}_r - \beta D\mathbf{H}(\mathbf{x})\boldsymbol{\xi}_i, \quad (9)$$

$$\dot{\boldsymbol{\xi}}_i = [D\mathbf{F}(\mathbf{x}) + \alpha D\mathbf{H}(\mathbf{x})]\boldsymbol{\xi}_i + \beta D\mathbf{H}(\mathbf{x})\boldsymbol{\xi}_r. \quad (10)$$

Given the coupling matrix $\mathbf{G}$, the transverse Lyapunov exponents can be estimated by solving Eqs. (9) and (10). The variations of the two maximum transverse Lyapunov exponents with ϵ can determine the transitions to synchronized states on different time-scale oscillations. Also, as in the two-neuron system, a similar analysis can be carried out for the network of N-coupled neurons by separating the dynamics into fast and slow subsystems. This theoretical approach precisely predicts the onset of burst synchrony in an N-neuron system (for example, the transition, $\epsilon_s \approx 0.11$, as observed in Fig. 5 for an eight-neuron system).

In summary, in a coupled multi-time-scale dynamical system of oscillators, we explore the effect of coupling strength on synchronization of the slow and fast subsystems. We find that neuronal synchrony of spike-burst activity is a multiscale phenomenon and involves synchrony of bursts and synchrony of spikes, or both. Coupling may not always decrease Lyapunov exponents. Instead, it does the opposite in a multiscale dynamical system such as coupled neurons, indicating that low values of coupling increase incoherence of oscillations. A stronger coupling synchronizes the system, but on two scales of oscillations. There is an order of synchrony onsets with increasing coupling value: first, synchrony on the slow time-scale oscillations (for example, burst synchrony) and then synchrony on the fast time-scale oscillations (spike synchrony).

This work was supported by DARPA Grant No. NBCH1020010, ONR Grant No. N00014-99-1, NIMH Grant No. MH64204, and NSF Grant No. IBN0090717.

[1] M. Steriade and R. R. Llinas, Physiol. Rev. **68**, 649 (1988).
[2] S. M. Sherman and C. Kock, Exp. Brain Res. **63**, 1 (1986).
[3] D. A. McCormick and H. R. Feeser, Neuroscience (N.Y.) **39**, 103 (1990).
[4] M. Steriade, D. A. McCormick, and T. J. Sejnowski, Science **262**, 679 (1993).
[5] F. Amzica and M. Steriade, Electroencephalogr. Clin. Neurophysiol. **2**, 69 (1998).
[6] W. Schultz, J. Neurophysiol. **80**, 1 (1998).
[7] A. S. Freeman, L. T. Meltzer, and B. S. Bunney, Life Sci. **36**, 1983 (1985).
[8] A. A. Grace and B. S. Bunney, Neuroscience (N.Y.) **10**, 2877 (1984).
[9] T. Ljungberg, P. Apicella, and W. Schultz, J. Neurophysiol. **67**, 145 (1992).
[10] D. R. Weinberger, Arch. Gen. Psychiatry **44**, 660 (1987).
[11] G. F. Koob, F. J. Vaccarino, M. Amalric, and F. E. Bloom, *Brain Reward Systems and Abuse*, edited by J. Engel and L. Oreland (Raven Press, New York, 1987), p. 35.
[12] M. Avoli, P. Gloor, G. Kostopoulos, and R. Naquet, *Generalized Epilepsy. Neurobiological Approaches* (Birkhauser, Boston, 1990).
[13] D. A. Hosford, S. Clark, Z. Cao, W. A. Wilson, F-H. Lin, R. A. Morisett, and A. Huin, Science **257**, 398 (1992).
[14] O. C. Snead, Ann. Neurol. **37**, 146 (1995).
[15] J. Rinzel and Y. S. Lee, J. Math. Biol. **25**, 653 (1987).
[16] E. M. Izhikevich, Int. J. Bifurcation Chaos Appl. Sci. Eng. **10**, 1171 (2000).
[17] L. M. Pecora and T. L. Carroll, Phys. Rev. Lett. **64**, 821 (1990).
[18] M. G. Rosenblum, A. S. Pikovsky, and J. Kurths, Phys. Rev. Lett. **76**, 1804 (1996).
[19] Z. Liu, Y.-C. Lai, and M. A. Matias, Phys. Rev. E **67**, 045203 (2003).
[20] J. L. Hindmarsh and R. M. Rose, Nature (London) **296**, 162 (1982).
[21] J. L. Hindmarsh and R. M. Rose, Proc. R. Soc. London, Ser. B **221**, 87 (1984).
[22] L. M. Pecora and T. L. Carroll, Phys. Rev. Lett. **80**, 2109 (1998).